# Convergent Gene Expression Patterns During Compatible Interactions Between Two *Pseudomonas syringae* Pathovars and a Common Host (*Nicotiana benthamiana*)

**Authors/Affiliations** (ORCID)

Morgan E. Carter, School of Plant Sciences, University of Arizona (0000-0001-5639-2013)

Amy Smith, Department of Plant Pathology, University of Georgia (0000-0001-9367-6453)

David A. Baltrus, School of Plant Sciences, University of Arizona (0000-0002-5166-9551)

Brian H. Kvitko, Department of Plant Pathology, University of Georgia (0000-0002-9094-4069)

**Contact Info**

Corresponding:

Baltrus@email.arizona.edu

bkvitko@uga.edu

## Summary/Abstract

*Pseudomonas syringae* is a diverse phytopathogenic species complex, and includes strains that can cause disease across a wide variety of plant species. Much previous research into the molecular basis of immunity and infection has focused on pathogen and plant responses in a handful of model strains and hosts, and with a tacit assumption that early steps in infection and host resistance are generalizable to the species complex and across plant hosts as a whole. Here, we provide a test of this assumption by measuring the dual pathogen and host transcriptomes of two distinct pathogenic lineages of *P. syringae* during compatible infection of a shared model host (*Nicotiana benthamiana*). Our results demonstrate that, with a handful of exceptions, host plants largely respond in a similar way to both pathogenic lineages at 5 hours post infection. This convergence in host responses occurs despite subtle but broader divergence in pathogen transcriptomes that hints at ecological differentiation during infection. Overall, our results provide evidence of common host responses to closely related pathogens while highlighting differential responses of distinct bacterial lineages during infection of a common host plant.

## Introduction

Knowledge of virulence mechanisms and strategies of phytopathogens has grown dramatically over the past few decades, largely due to a focus on gaining a deep understanding of infection in a handful of well vetted and tractable strains and host plants. As one steps out to lesser studied strains and hosts, it is often assumed that relatively closely related bacterial phytopathogens use similar virulence pathways and strategies to overcome host defenses to cause disease. While such assumptions are rightly borne out of a desire for experimental efficiency and often hold up to scrutiny, they nonetheless remain fundamental assumptions until proven otherwise even if pathogens differ in timing and symptom development across hosts. With this idea in mind, we sought to categorize similarities and differences in responses of a common host plant to closely related bacterial phytopathogens during the early stages of infection under compatible interactions.

*Pseudomonas syringae* sensu lato consists of a collection of bacterial phytopathogens spanning a variety of formal species names and which is composed of upwards of 50 different pathovars (Susan S. Hirano and Upper 2000; Baltrus, McCann, and Guttman 2017). Pathovar designation for *P. syringae* sensu lato strains is typically designated based on phenotypic information such as host of isolation and more recently informed by genotypic, genomic, and phylogenetic characteristics (Baltrus, McCann, and Guttman 2017; Baltrus 2016). Much research effort has been spent to develop multiple *P. syringae* strains as model systems for virulence in a variety of host plants and these studies have been foundational for understanding bacterial virulence strategies as well host resistance to these pathogens (Lindeberg et al. 2006; Block and Alfano 2011; Xin, Kvitko, and He 2018). However, despite the incredible accumulation of data about biology and genomics of specific *P. syringae* strains, much of our understanding of virulence patterns remains dependent on assumptions of similarity of virulence strategies across various pathovars within the *P. syringae* sensu lato complex or is integrated across interactions between pathovars and diverse hosts. We therefore sought to compare and contrast host plant responses and the infection strategies across two *P. syringae* strains that can each infect and cause disease (albeit within different symptoms) on *Nicotiana benthamiana*.

We focused on two closely related strains for this study: *P. syringae* pv. *syringae* B728a (hereafter *Psy*) and *P. amygdali* pv. *tabaci* 11528 (hereafter *Pta). Psy* is a member of phylogroup 2 and was originally isolated as the causative agent of brown spot disease in common bean plants (*Phaseolus vulgaris*), and is well studied for its capabilities of survival as a plant epiphyte and and as a pathogen of numerous hosts (Feil et al. 2005; Helmann, Deutschbauer, and Lindow 2019; Baltrus, McCann, and Guttman 2017). *Pta* is a member of phylogroup 3 and was originally isolated as the causative agent of wildfire disease in tobacco plants (*Nicotiana tabacum)* but has also been reported to cause similar disease across bean hosts (Sun et al. 2021; Baltrus, McCann, and Guttman 2017). Previous genomic comparisons of these strains in the context of *P. syringae* diversity have suggested that these strains may differ in virulence strategies (Baltrus et al. 2011; Hockett et al. 2014); while a type III secretion system is critical for infection of hosts by both

strains (S. S. Hirano et al. 1999) the effector repertoire of phylogroup 2 strains including *Psy* (16 effectors) appears reduced compared to that of many other analyzed strains with this reduction strongly correlated with acquisition of a suite of phytotoxins (syringomycin, syringopeptin, and syringolin) (Hockett et al. 2014; Baltrus et al. 2011). *Pta* shares 8 effectors with *Psy* and maintains a slightly larger repertoire than *Psy* (18 unique effectors and 21 total, reannotated herein), but also contains a different suite of phytotoxins (tabtoxin and phevamine). Despite the potential for differences in virulence strategies, to date there have been no direct comparisons of host responses to these strains during compatible infection.

We investigated the two compatible disease interactions between *N. benthamiana* and *Psy* or *Pta* at the early time point of five hours post inoculation to understand how a plant host responds to two related bacteria with different infection strategies. There was clear overlap in the differentially expressed genes in response to both pathogens, but also clear transcriptome responses related to hormones and chloroplasts that were specific to one infection or the other. By identifying orthologous genes in *Pta* and *Psy*, we determined they do both upregulate the type III secretion system and many effector genes but do not share common differential expression in genes related to motility and alginate production at this stage *in planta*.

## Results

### *A complete genome sequence for P. syringae pv. tabaci ATCC11528 and reannotation of virulence factors*

We and others have previously reported draft genome assemblies for *P. syringae* pv. tabaci strain ATCC11528 (Baltrus et al. 2011; Studholme et al. 2009), and here we report a complete genome assembled using a hybrid strategy that combined Illumina and Nanopore reads. The genome contains one circular chromosome that is 6,133,558 bp (Genbank accession CP042804.1) and one 68,162 circular plasmid (Genbank accession CP042805.1) which we name pTab1. The genome is predicted to encode a total of 5,488 proteins, 66 tRNA loci, 5 complete rRNA operons and 4 other non-coding RNA. We have used this genome sequence to reanalyze and revise annotations of type III effector proteins and their regulatory *hrp*-boxes. These annotations can be found in an associated file on Figshare at doi: 10.6084/m9.figshare.20151770

We have used the complete genome sequence for strain *Pta* to update annotations and positions of known virulence factors. We previously noted *hopR* and *hop*AB as possibly truncated and/or incomplete (Baltrus et al. 2011), and this was shown to be an error when different versions of this genome were reported. We note here that both *hopR* and *hopAB* appear to be full length and non-truncated in this complete genome assembly. We have confirmed that *hopAA1*, *hopAH1*, and *hopAI1* all appear to be truncated via nonsense mutations within this complete genome. Lastly, we find that this genome contains four identical copies of the effector *hopW*, denoted *hop*W1-1 through *hop*W1-4 in different positions throughout the chromosome and plasmid. Indeed, *hop*W1-4 is the only type III effector found on plasmid pTab1. In total, this strain is predicted to encode 18 full length type III effectors. We also note positions of the two phytotoxins known or predicted to be produced by this strain. Tabtoxin production is determined

by two separate operons found in proximity to each other on the genome. However, surprisingly, we find that there are two regions of the chromosome that contain genes implicated in producing phevamine and that these two regions are identical in nucleotide sequence. We have labeled the first phevamine operon 1, and refer to these three genes as *hsv*1-1, *hsv*2-1, and *hsv*3-1. Genes within the second phevamine operon are labeled as *hsv*1-2, *hsv*2-2, and *hsv*3-2.

*RNA-seq analysis showed differential expression in response to both pathogens*

RNA was collected and sequenced from two sets of *N. benthamiana* plants before inoculation and five hours post inoculation (hpi) with either *Pta* or *Psy*. Transcriptomes were compared for plants before and after inoculation and the threshold for differential expression was set at an adjusted p-value (padj) of 0.01 and an absolute value of the Log2 Fold Change (L2FC) above 2 (**Figure 1A**, **Supplemental Figure 1, Supplemental Table 1**). A set of 2245 genes (**Figure 1B**) are differentially expressed (DE) in response to both pathogens at 5 hpi. While the 5 hpi time point represents genes with transcriptional responses both to infection by the *Pseudomonas* pathogens and to the short passage of time, making it difficult to attribute changes to one variable or the other, we still observed informative trends. Gene ontology (GO) enrichment analysis yielded 138 enriched GO terms in the shared DE genes (**Supplemental Figure 2**). The top eight enriched biological processes (BP) GO terms are related to photosynthesis and the response to light, with the associated genes being largely downregulated (**Figure 2**).

"Response to" GO terms for stresses are also enriched in the shared DE genes (**Figure 2**) including defense response to fungus (GO:0050832), response to cold (GO:0009409), response of abscisic acid (GO:0009737), and both response to water deprivation (GO:0009414) and response to water (GO:0009415). In contrast to the photosynthesis-related DE genes, those annotated with "response to" GO terms are often upregulated as expected by the introduction of a biotic stress. Other terms of interest related to known aspects of pathogenesis and defense include regulation of stomatal movement (GO:0010119) and oxylipin biosynthetic processes (GO:0031408); the plant hormone jasmonic acid and other oxylipins play a large role in plant development and stress response (Creelman and Mulpuri 2002). A PR1 ortholog (NbD052315) is highly downregulated in both ($L2FC_{Psy}$=-11.65, $L2FC_{Pta}$=-9.94); PR1 is widely used as a salicylic acid pathway molecular marker. Further changes in metabolism-related genes likely increase sesquiterpene biosynthesis (GO:0051762) through multiple upregulated sesquiterpene synthases and 5-epi-aristolochene synthase-like genes, as well as changes in flavonoid biosynthesis (GO:0009813) through up- and downregulated glycosyltransferases.

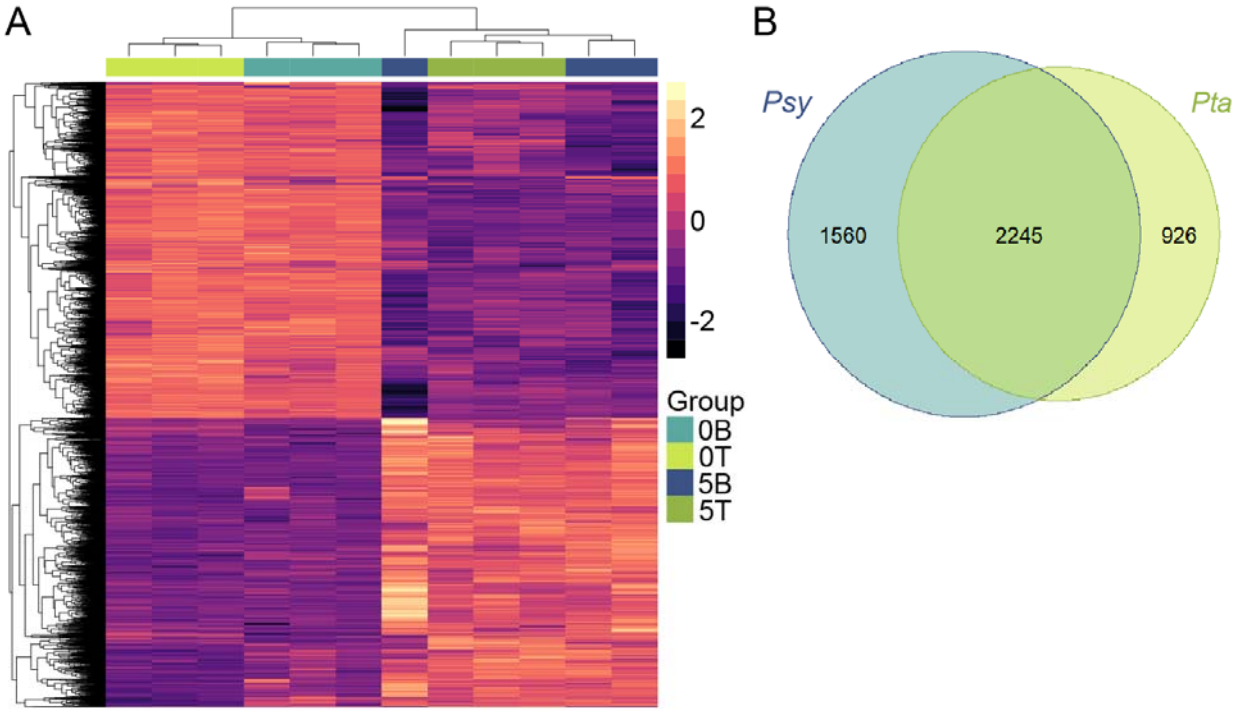


**Figure 1**. Differentially expressed genes in *Nicotiana benthamiana* in response to inoculation with *Psy* or *Pta* five hours post inoculation. (A) Heat map showing regularized logarithm transformation of the count data for genes that are differentially expressed in response to *Pta* or *Psy* or both. 0B, uninoculated; 0T, uninoculated; 5B, 0B plants 5 hpi with *Psy*, 5T, 0T plants 5 hpi with *Pta*. (B) Venn Diagram showing total genes differentially expressed in response to *Pta* or *Psy* or both.

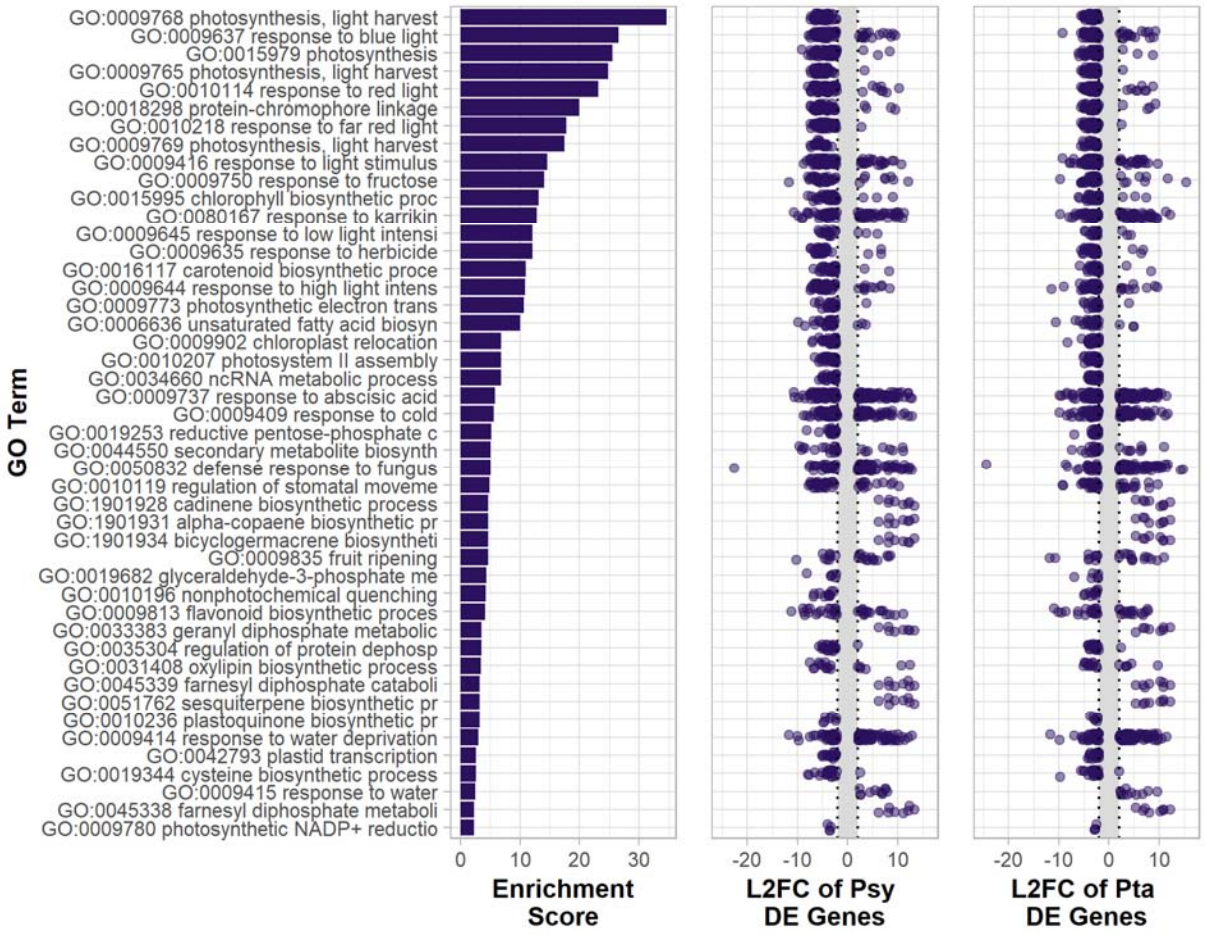


**Figure 2.** Gene ontology (GO) enrichment for differentially expressed (DE) genes shared in the responses of *Nicotiana benthamiana* to inoculation with *Psy* or *Pta* at 5 hpi. All GO terms depicted are from the category biological processes and have an adjusted *p* value<0.01. A complete list of enriched GO terms is shown in Supplemental Figure 2. L2FC, $\log_2$ fold change.

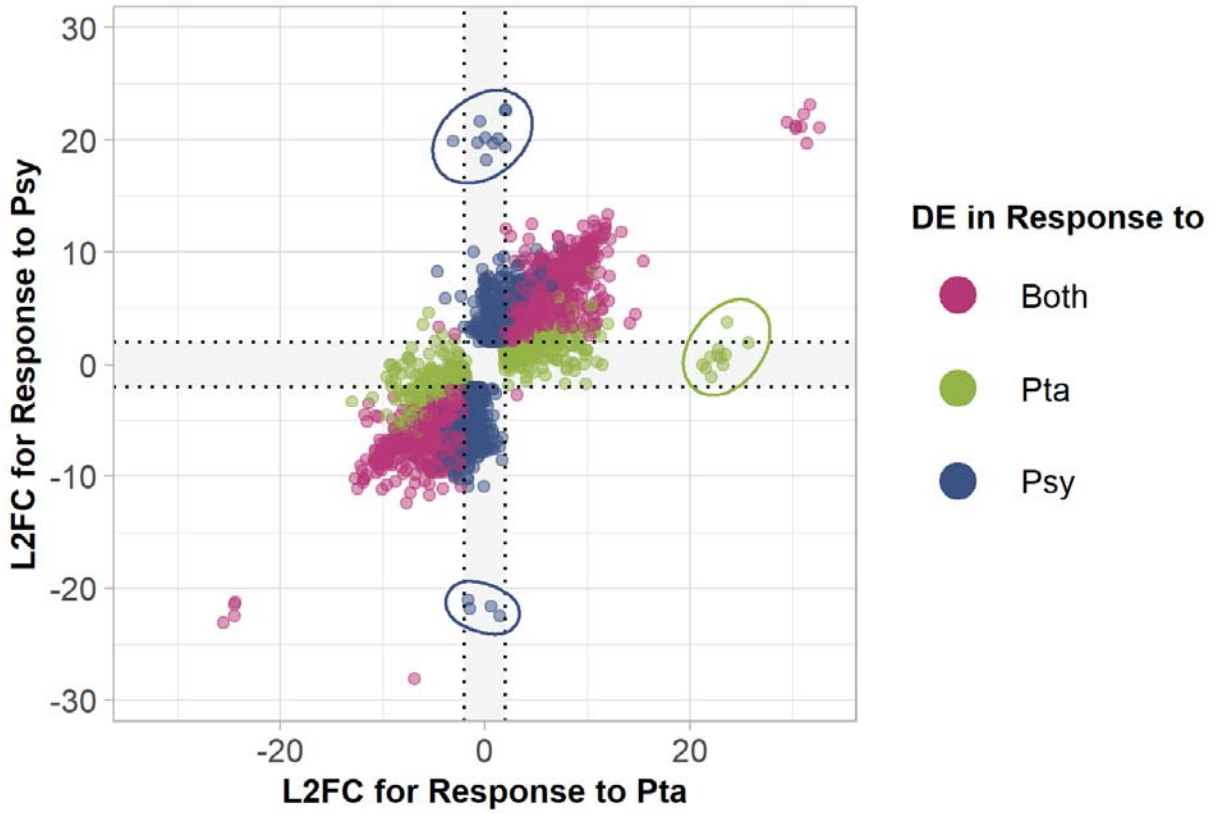


**Figure 3**. Scatterplot of the *Nicotiana benthamiana* genes that are differentially expressed (DE) in response to *Psy*, *Pta*, or both. The axes represent that $\log_2$ fold change (L2FC) of the genes in response to one pathogen or the other. The circles indicate the most DE genes in response to one pathogen that are listed in **Tables 1 and 2**.

*Response to* Psy *involves more chloroplast-related genes*

We chose to focus the rest of our inquiry on the 1560 and 926 genes DE only in response to infection with *Psy* or *Pta*, respectively (**Figure 1B, Figure 3**). In response to *Psy*, 651 genes are upregulated and 909 are downregulated. Of the ten DE genes with a L2FC>15 in response to *Psy* (**Table 1**), three are related to auxin response and homeostasis (NbD025458, NbD037056, and NbD041542). NbD025458, the highest upregulated, codes for a putative CHD3/CHD4-like chromatin remodeling protein, while the second highest, NbD037056, is a BIG auxin transport protein. Eleven other upregulated genes are predicted IAA/Aux or auxin response factor (ARF) transcriptional activators or repressors. Overall, 60 upregulated genes have auxin-related GO terms; 46 auxin-related genes are downregulated, including some related to brassinosteroid and abscisic acid signaling such as orthologs of HAT1, PILS5, and TTL1. NbD041542 is a Protein DETOXIFICATION 48 homolog, a multidrug and toxin extrusion transporter that can mediate iron homeostasis under stress (Seo et al. 2012). An additional upregulated gene is a putative callose synthase (NbD005055), but only certain callose synthases are important for plant defense, with others involved in development and division and plasmodesmatal permeability control (Ellinger and Voigt 2014; Wu et al. 2018). NbD005055 was computationally predicted as

callose synthase 1- or 2-like, which are both known to be induced are part of the defense response to pathogens in Arabidopsis in a salicylic acid-dependent manner (Dong et al. 2008), but are also described as serving roles in cell division (Ellinger and Voigt 2014). The four most downregulated genes are mostly uncharacterized, though one (NbD033797) has homology to a soybean transcription factor and another (NbD000103) is related to a positive regulator of floral development in Arabidopsis (Murtas et al. 2003).

**Table 1**. Genes differentially expressed in response to *Psy* at 5 hpi with an absolute value of $\log_2$ fold change (L2FC) greater than 15.

| Gene | Product | Gene Name* | Description* | L2FC |
|---|---|---|---|---|
| NbD025458 | uncharacterized protein LOC104212182 | chd4 | CHD3-type chromatin-remodeling factor PICKLE | 22.61 |
| NbD037056 | auxin transport protein BIG isoform X1 | BIG | Auxin transport protein BIG | 22.60 |
| NbD010045 | ribosomal protein S13 (mitochondrion) | rps13 | Ribosomal protein S13 | 21.65 |
| NbD005055 | callose synthase 2-like | CALS1 | Callose synthase 1 | 20.20 |
| NbD042013 | cleavage and polyadenylation specificity factor subunit 3-II | FEG | Integrator complex subunit 11 | 20.09 |
| NbD031078 | uncharacterized protein LOC109215177 | At2g38970 | C3HC4-type RING finger-containing protein | 19.89 |
| NbD052852 | ubiquitin-conjugating enzyme E2 variant 1C-like, partial | UEV1D | Ubiquitin-conjugating enzyme E2 variant 1D | 19.76 |
| NbD026296 | MAP3K epsilon protein kinase 1-like | M3KE1 | MAP3K epsilon protein kinase 1 | 19.70 |
| NbD041542 | protein DETOXIFICATION 48-like | DTX48 | Protein DETOXIFICATION 48 | 19.42 |
| NbD032348 | rho GTPase-activating protein 7-like isoform X1 | ROPGAP7 | Rho GTPase-activating protein 7 | 18.17 |
| NbD020455 | Partial, uncharacterized protein LOC109226839 | - | - | -21.06 |
| NbD000103 | Partial, ubiquitin-like-specific protease ESD4 | ESD4 | Ubiquitin-like-specific protease ESD4 | -21.68 |
| NbD019312 | uncharacterized protein LOC104238947 | At1g12380 | F5O11.10 | -21.88 |

| | | | | |
|---|---|---|---|---|
| NbD033797 | uncharacterized protein LOC107824489 | glysoja_046371 | Transcription factor, putative | -22.46 |

**UniRef90 BLAST top hit as annotated by Sma3s v2*

In a clear trend, genes DE in response to *Psy* were enriched for GO terms relating to chloroplasts (**Figure 4**), including the top three cellular component (CC) terms of chloroplast envelope (GO:0009941), chloroplast (GO:0009507), and chloroplast thylakoid membrane (GO:0009535). Of the 1560 DE genes, 380 of them have enriched chloroplast-related CC GO terms and of those, 326 are downregulated. Four of the 54 upregulated genes are related to glutathione redox signaling; two glutathione S-transferases (NbD007461, NbD045751), glutathione reductase (gr;NbD022932), and glutathione peroxidase (gpx; NbD036458). The most upregulated gene with the chloroplast envelope GO term is a 9-divinyl ether synthase (DES; NbD030668); under biotic stress, related proteins can form antimicrobial oxylipins that have been found to be more useful against eukaryotic pathogens (Prost et al. 2005). For example, NtDES1 from *N. tabacum* is upregulated in the early response to a pathogenic oomycete, while other oxylipin synthesis genes have roles in defense against nematode and fungal infections (Fammartino et al. 2007; Wang et al. 2021; Sanadhya et al. 2021). In contrast, the most downregulated gene with the chloroplast envelope GO term is a receptor-like kinase (NbD047510) from the THESEUS 1/FERONIA family that can serve to detect cell wall defects and damage (Cheung and Wu 2011); this gene is annotated with additional GO terms associated with other cellular membranes, indicating unclear predicted localization.

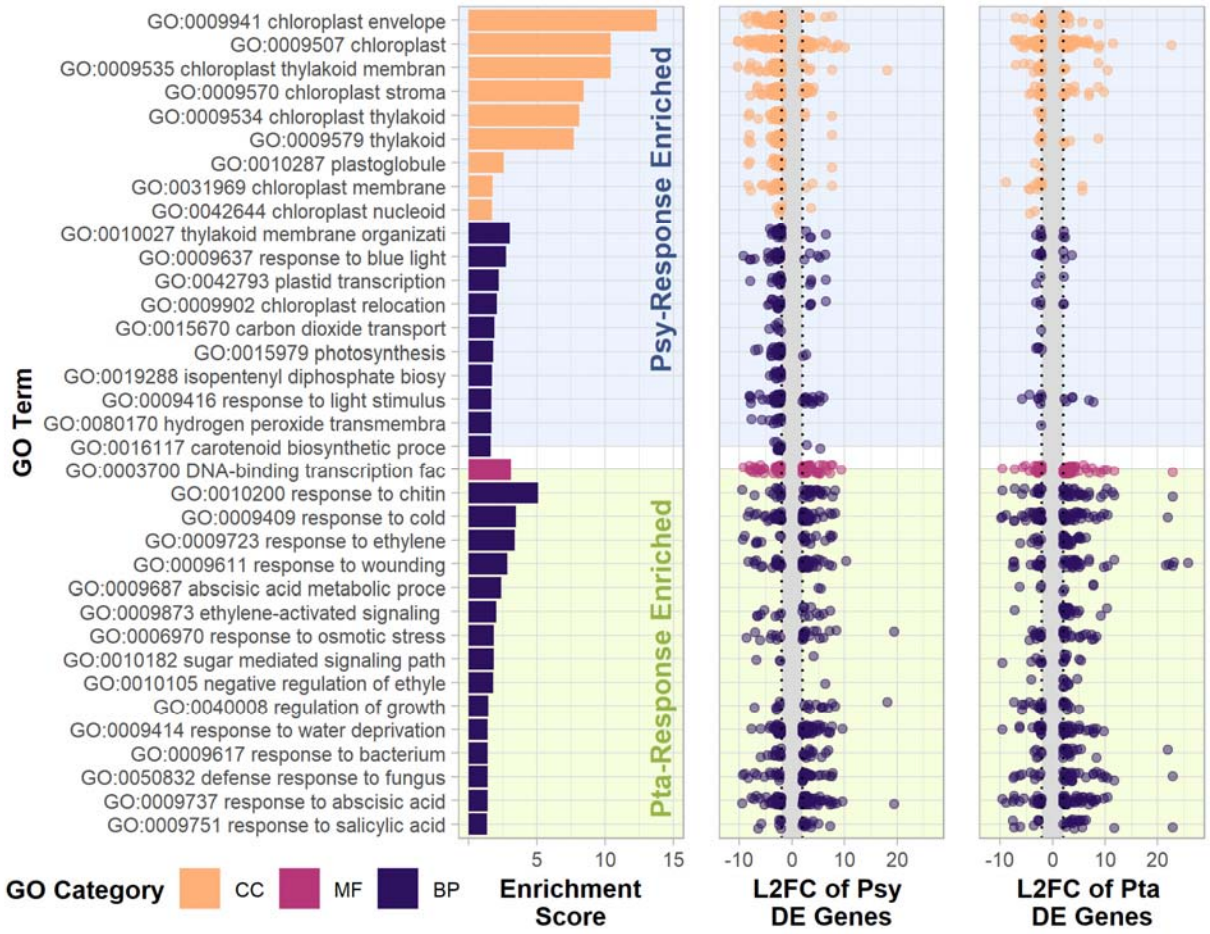


**Figure 4.** Gene ontology (GO) enrichment for differentially expressed (DE) genes specific to the response of *Nicotiana benthamiana* to inoculation with *Psy* or with *Pta* at 5 hpi. GO terms were considered enriched for an adjusted *p* value<0.05. L2FC, $\log_2$ fold change; CC, cellular component; MF, molecular function; BP, biological processes.

*Response to* Pta *involves more hormone and calcium signaling*

In total, 489 genes were upregulated and 437 downregulated specifically in response to *Pta* infection. Of the most DE genes (**Figure 3**), three are calcium binding proteins and two are cytochrome P450s (**Table 2**). Related cytochrome P450s CYP94B1, CYP95B3, and CYP94A1 regulate and interact with jasmonic acid signaling in Arabidopsis and *Vicia sativa* (Koo et al. 2014; Pinot et al. 1998; Heitz et al. 2012). Calcium signaling positively and negatively regulates the response to plant pathogens via calcium binding proteins like calmodulin (Zhang, Du, and Poovaiah 2014). For example, cellular calcium ion concentration changes can lead to negative regulation of the salicylic acid pathway by downregulating gene expression of EDS1 by AtSR1, dependent on calmodulin binding (Du et al. 2009). Virulent *P. syringae* pv. *tomato* can increase intracellular calcium, resulting in downregulation of salicylic acid receptor NPR1 by AtSR1, as well (Yuan, Tanaka, and Poovaiah 2021). Though, these calcium-binding proteins may be

serving other roles, as an EDS1 homolog (NbD037498) and two NPR3 homologs (NbD049359, NbD051607) are upregulated by a L2FC of 2.7 to 4 in the shared response, or response to *Psy* for NbD051607. Another of the most DE genes is a nucleotide-binding leucine-rich repeat protein (NbD051268), a class of resistance proteins involved in pathogen perception and defense; this one must not confer resistance to these *Pseudomonas* strains given the compatibility for disease progression.

**Table 2**.Genes differentially expressed in response to *Pta* at 5 hpi with an absolute value of $\log_2$ fold change (L2FC) greater than 15.

| Gene | Product | Gene Name* | Description* | L2FC |
|---|---|---|---|---|
| NbD046869 | regulator of gene silencing | CML38 | Calcium-binding protein CML38 | 25.79 |
| NbD051268 | putative late blight resistance protein homolog R1B-16 isoform X1 | | NBS resistance protein RGA41 | 23.64 |
| NbD002038 | protein MOR1 | MOR1 | Protein MOR1 | 23.53 |
| NbD014197 | cytochrome P450 94B3-like | CYP94B1 | Cytochrome P450 94B1 | 23.15 |
| NbD006192 | probable WRKY transcription factor 40 | wizz | WIZZ | 22.90 |
| NbD005810 | Partial, ribosomal protein S2 (chloroplast) | rps | 30S ribosomal protein S2, chloroplastic | 22.70 |
| NbD022237 | probable calcium-binding protein CML13 | zbf3 | Calmodulin | 22.58 |
| NbD001244 | putative calcium-binding protein CML19 | CML19 | Putative calcium-binding protein CML19 | 22.15 |
| NbD000167 | glucan endo-1,3-beta-glucosidase, acidic isoform GI9-like | PR2 | Glucan endo-1,3-beta-glucosidase, acidic isoform GI9 | 21.94 |
| NbD000127 | Partial, cytochrome P450 94B3-like | CYP450A | Cytochrome P450 94A1 | 21.58 |
| NbD017845 | uncharacterized protein LOC108946890 | ORFIII | Polyprotein III | 21.28 |

**UniRef90 BLAST top hit as annotated by Sma3s v2*

In contrast to the response to *Psy*, there are no enriched CC GO terms (**Figure 4**) in the DE genes specific to the *Pta* infection response. The majority of the enriched BP GO terms are

for responses to biotic and abiotic stresses with the top three being response to chitin (GO:0010200), response to cold (GO:0009409), and response to ethylene (GO:0009723). Of the 51 DE genes with ethylene-related enriched GO terms (GO:0009723, GO:0009873, GO:0010105), 41 are upregulated and 9 are downregulated. Among the upregulated genes are two putative RMA1H1-like E3 ubiquitin-protein ligases, which inhibit aquaporin trafficking during drought stress in hot pepper (Lee et al. 2009). Many upregulated ethylene response genes included transcription factors ilike orthologs of ERF1, ERF2, ERF3, ERF4, ERF5, ERF011, EIN3, EIN4, and RAV1. In fact, putative transcription factors (TF) are generally enriched in the upregulated genes in response to *Pta* as indicated by the molecular function (MF) GO term DNA-binding transcription factor (GO:0003700). Beyond the ethylene-response TFs, two orthologs of the wound-response TF WIZZ (Hara et al. 2000) are highly upregulated, followed by zinc-finger binding proteins and two orthologs of fungal-response TF WRKY33 (Zheng et al. 2006).

*Bacterial virulence genes typically followed expected expression patterns* in planta

In parallel, we assessed the changes in gene expression within the bacteria, identifying orthologous pairs to compare and contrast their virulence strategies. *Psy* and *Pta* differentially express 101 orthologous genes (**Fig. 5**) five hours post infection *in planta* compared to growth on solid agar. An additional 610 orthologous genes and 141 unique genes are DE in *Pta*, and 248 and 84 in *Psy*, respectively. The type III secretion system is one of the most important pathways involved for virulence *in planta* for *Pseudomonas syringae*, and many structural and regulatory components of this pathway are differentially expressed genes across both pathogens *in planta* (**Fig. 6**). Likewise, many effector proteins that are known to be translocated across the type III secretion system are also either differentially upregulated or trend in that direction for both *Psy* and *Pta*, including nine shared effector proteins (*avrE*, *hopM*, *hopI*, *hopAG1*, *hopAE1*, *hopAB1*, *hopX1*, and although truncated in *Pta*, *hopAH1* and *hopAA1*). This is of note because, although *hopAH2* populates many effector lists, the effector status of this locus has been long questioned given that it does not have a clearly identifiable *hrp* box in *Psy* although it is capable of being delivered via the T3SS. Most of the effector genes that are uniquely found in one pathogen but not the other are also either differentially expressed or trend that way with one interesting exception. *hop*W1 is found in four identical copies throughout the genome of *Pta*, including one copy present on a plasmid. However, although precise measurement of expression differences for these loci is difficult because of multimapping to identical sequences, it does not appear that any of these *hopW1* loci are differentially expressed *in planta* in *Pta* when considered individually.

These two pathogenic strains do not share phytotoxin pathways, but we find that each of these pathways also appear to be largely upregulated *in planta* at 5hpi. For instance, all known phytotoxins in *Psy* are differentially upregulated *in planta* at 5 hpi. These include pathways for syringomycin production (*syr*B1, *syr*B2, *syr*CDEF), syringopeptin production (*syp*ABC) and syringolin production and export (*syl*ABCDE, *pse*ABC). Likewise, there are two copies of the operon predicted to encode phevamine A in *Pta*, and all of the genes in each (*hsv*ABC) are highly upregulated. Surprisingly, however, we find that loci involved in the regulation and production of tabtoxin (*tab*ABCDP, *tbl*ACDEFRS*)* are all significantly downregulated *in planta* compared to growth on solid agar.

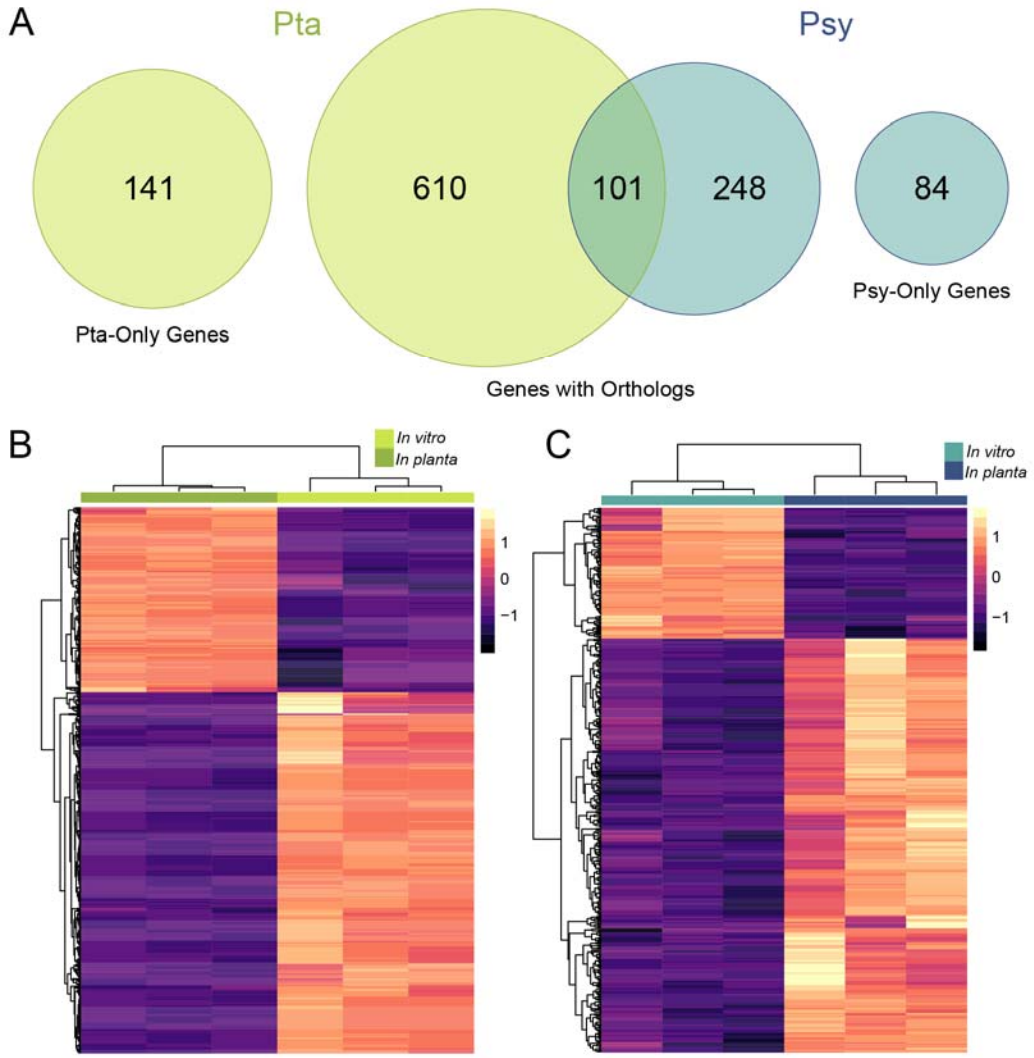


**Figure 5.** Differential gene expression in *Pseudomonas* strains *in vitro* compared to *in planta* five hours post inoculation. (A) Venn diagram depicting the number of differentially expressed genes with and without orthologs in *Pta* and *Psy*. (B-C) Heat map showing regularized logarithm transformation of the count data for genes that are differentially expressed by (B) *Pta* and (C) *Psy* during early plant infection

Bacterial Expression Responses of Additional Genes *In Planta*

There is a dominant overall signal of growth differences for both strains *in planta* compared to on solid agar. This signal is represented as a variety of "housekeeping" genes involved in basic growth processes like cell division and translation being differentially expressed during infection, and somewhat obscures our ability to identify "newly" expressed genes *in planta* because these could likely just represent correlates of growth. There do exist a variety of virulence adjacent pathways that are differentially expressed, which are oppositely

expressed across both pathogen genomes, or where regulation is known to be independent of growth that are worth highlighting between both strains. In particular, the genes that differ or contrast each other in expression between these strains could reflect true biological differences between strains and may provide insights into differences in disease etiology or progression. Notably, genes involved in both flagellar and pili-based motility are downregulated in *Pta* during infection but are largely unchanged or slightly trend towards downregulated for these same conditions in *Psy* (**Figure 6**). Genes involved in alginate production are largely upregulated during infection with *Psy* while there is a trend towards downregulation in *Pta*. Lastly, operons involved in the production of phage derived tailocin molecules (PSYTB_RS25445 to PSYTB_RS25575) are strongly upregulated in *Pta* while this same operon (Psyr_4582 to Psyr_4608) is either unchanged or trends towards downregulated in *Psy* (**Supplemental Figure S4**).

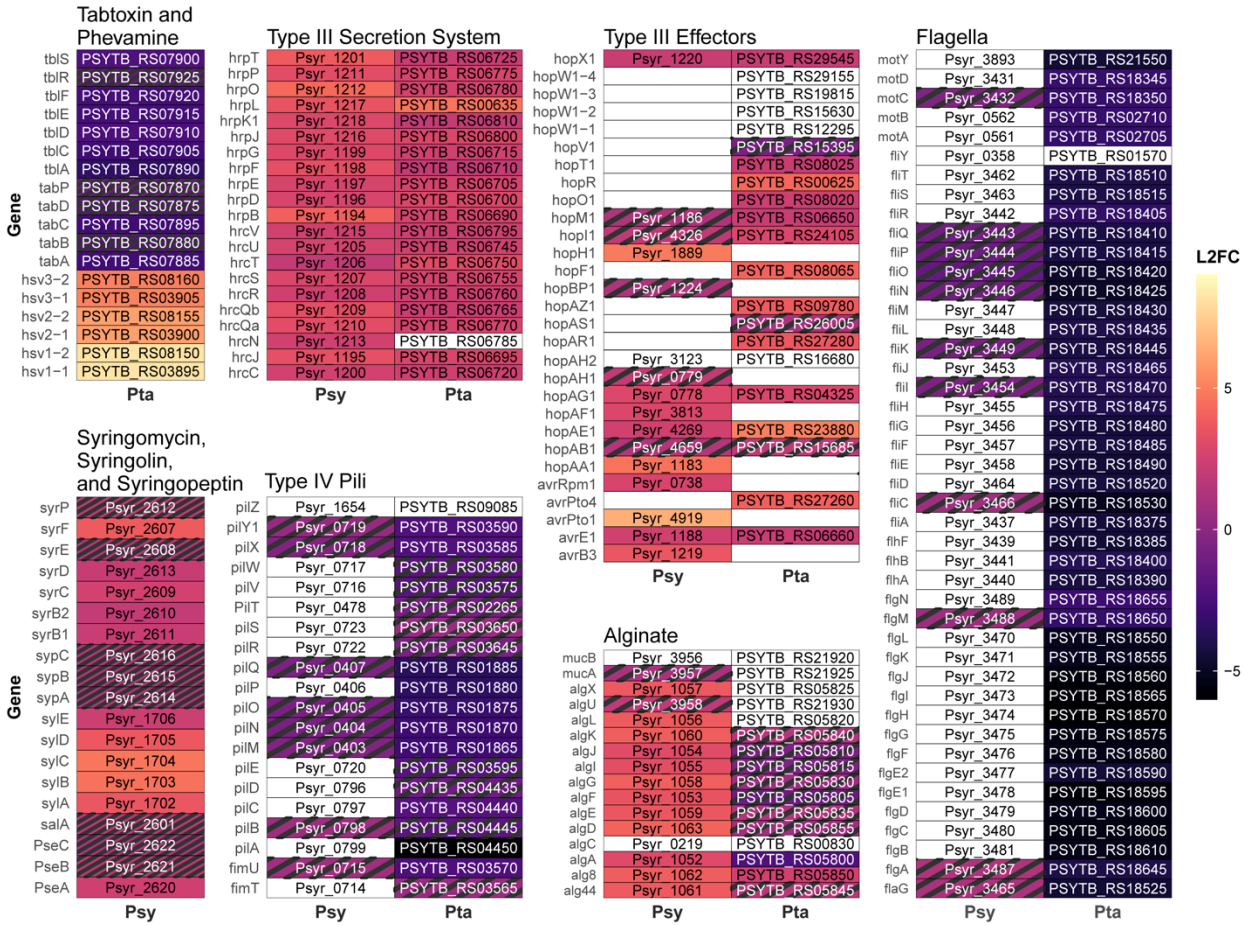


**Figure 6**. Differential expression of select virulence-related genes and pathways in *Psy* and *Pta in planta*. Striped boxes indicate genes that are significant for different thresholds: adjusted p value<0.05 and no minimum $\log_2$ fold change (L2FC). White boxes indicate no ortholog present or, when labeled with a locus ID, orthologs that are not differentially expressed.

## Discussion

Extensive research over numerous decades has enabled fine scale characterization of the genetic basis of the variety of overlapping defense responses used by plants to defend against bacterial pathogens. Along the same lines, diverse arsenals used by various pathogens to overcome these defense responses have also been detailed using established model systems across plant hosts, with research highlighting the many ways that bacteria can disrupt plant host defenses. However, there has been relatively less emphasis on comparing and contrasting the genetic basis of compatible infections (where the outcome is disease) within a single host during infection by divergent phytopathogens, although responses are largely assumed to be correlated with overcoming common defense pathways.

Here, we report host responses during infection of *Nicotiana benthamiana* with two relatively closely related phytopathogens that cause different diseases under natural conditions. While both pathogens (*Pseudomonas syringae* pv. syringae B728a, *Psy*; *Pseudomonas amygdali* pv. tabaci ATCC11528, *Pta*) fall under the banner of *Pseudomonas syringae* senso lato, they are classified as different phylogroups and species and potentially rely on different suites of virulence genes during compatible interactions (Baltrus et al. 2011). *Pta* is the causative agent of tobacco wildfire disease, and is thought to rely on a large number of type III effectors (18) as well as the tabtoxin and phevamine for growth and disease *in planta* (Baltrus et al. 2011; Studholme et al. 2009; O'Neill et al. 2018). *Psy* is the causative agent of brown spot of bean, and possesses fewer effectors than *Pta* (16) in addition to three different phytotoxins (syringomycin, syringolin, syringopeptin) (Feil et al. 2005; Helmann, Deutschbauer, and Lindow 2019; Vinatzer et al. 2006).

At a broad stroke, as reflected in Figs. 1, 2, and 3, plant responses to both pathogens are similar, with highly correlated levels of expression changes of the host plants to both pathogens. Notably, there are significantly different expression levels occurring in numerous pathways known to be involved in plant defense and both pathogens induce dramatic changes in chloroplast gene expression. We also note that, while it is possible that both pathogens are directly targeting and manipulating a subset or all of these pathways to cause disease, we cannot rule out that that these expression changes are also akin to a plant SOS message and are the product of general levels of stress as the internal plant environment degrades during infection. Despite perceived differences in virulence potential based on presence and absence of virulence factors across the *Psy* and *Pta* genomes, it does appear that infection by either pathogen tends to converge on similar changes within the host and that perceived differences in virulence strategies by the pathogen largely lead to similar outcomes, at least at these early interaction time points.

A subset of host responses significantly differs between the two pathogens, and these differences could signal more subtle divergence in virulence strategies between the pathogens themselves. Infection responses to *Psy* appear to lean more heavily on changes in chloroplast gene expression, while pathways that respond to *Pta* are biased towards those involved in response to regulation by plant hormones. As per Fig. 3, it is likely that all of these pathways

generally respond in a similar way to both pathogens, but that effect sizes and variances across replicates of the responses are skewed in a way that yields statistical significance in only one of the two. It is also possible that these more subtle differences in response speak towards differences in the timing of infection. Since our sampling scheme had a standard time frame (5 hours post infection), it may be that both pathogens differ in when they affect common pathways and that these differences are being picked up in our larger analyses as strain specific responses.

Perhaps most interesting are genes in which expression changes significantly in response to one of the pathogens but which are virtually unchanged in the other pathogen (circled in Figure 3 and listed in Tables 1 and 2). Unlike many of the other genes that change significantly in response to infection in a correlated way between the two pathogens, and which therefore fall close to the diagonal in Figure 3, the circled genes are clearly biased in response to one of the pathogens. As above, these trends could reflect subtle timing differences between the pathogens during infection and thus might be significantly changed in both pathogens if measured at a different time scale. However, of any of the responses shown here, this class of genes is also the most likely to be responsive to only one of the pathogens and may reflect the outcomes of specific mechanisms of virulence employed by that strain. These genes also involve numerous loci that could be implicated in plant defense responses including pathways involved in callose production, ubiquitin ligases and proteases, MAP3K kinase and a WRKY transcription factor, calcium binding proteins, an NBS resistance protein, as well as a handful of uncharacterized proteins that will be interesting targets for future research efforts.

Prior to the experiments reported herein, and although we could make educated guesses based on previous research, it was unknown how similar (or different) a host plant's responses to infection by two relatively closely related pathogens would be. We can now say that, at least for these two strains, that overall responses are broadly very similar across infection with these two pathogens at an early time point. Many of the significant differences are differences in magnitude but not in trend, and can potentially be explained by differences in the timing of disease development between these strains. This convergence in host responses occurs despite divergence in the virulence arsenal between strains (both in terms of type III effectors and toxins). Conversely, there are a handful of genes that appear to be clearly and truly changed in regulation in response to one pathogen but not the other, and these genes are the best candidates for being the targets of strain specific virulence factors and potentially underlie or reflect the differences in disease phenotypes for these pathogens.

Comparison of gene expression signatures across these two bacterial strains offers a more complex story. The type III secretion system and effector proteins translocated by this system are thought critical for virulence of diverse *P. syringae* strains that infect diverse host plants. As expected, we find that many of the structural proteins involved in type III secretion and annotated type III effector proteins identified in each strain are upregulated at five hours post infection. These include effectors that are shared between both genomes as well as those that are exclusive to only one of the genomes. Expression of type III effectors is thought to be largely dependent on the action of the sigma factor HrpL, which binds to *hrp* boxes to recruit RNA polymerase to these regulons (Xiao and Hutcheson 1994; Ferreira et al. 2006; Lam et al. 2014).

As part of this study, we have identified potential *hrp* boxes upstream of effector proteins and all effector loci identifed as upregulated *in planta* are located downstream of a potential *hrp* box promoter with the exception of Psy *hopBP1* (aka hopZ3). Both strains also contain phytotoxins that are demonstrated virulence factors. All three phytotoxins in *Psy* (syringomycin, syringopeptin, syringolin) are upregulated at 5 hpi compared to the controls. This suggests that, although toxins like syringolin have been shown to function to prevent stomatal closure to initiate infection (Schellenberg, Ramel, and Dudler 2010), they could also carry out numerous additional virulence functions. Likewise, the small molecule phevamine A has been shown to dampen plant immune responses to compatible pathogens (O'Neill et al. 2018). The phevamine A production operon is duplicated in *Pta*, but both copies appear to be relatively highly expressed in this pathogen *in planta*. However, in stark contrast to these other results, all genes implicated in tabtoxin production in *Pta* appear to be downregulated at 5 hpi *in planta*. While it is possible that tabtoxin is a virulence factor that contributes during early stages of infection, it remains a possibility that this toxin contributes to late virulence *in planta* or only under certain environmental conditions or in certain hosts. Indeed, this line of thinking would be in line with a molecular version of the well-known "disease triangle" framework.

We also highlight that, since many of the predicted virulence genes are upregulated and correlated in expression between in both pathogens at the time point measured, that any differences in expression of other pathways represents a true divergence in expression profiles and is not simply a correlate of the environment that strains may be experiencing differently. To this point, although strain *Psy* has been demonstrated to systemically travel throughout *Nicotiana* plants during infection (Misas-Villamil, Kolodziejek, and van der Hoorn 2011), we find that all genes implicated in flagellar and pili based motility within this pathogen are largely unchanged in expression at 5 hpi (although they trend towards downregulated). Conversely, almost all of the genes contributing to both types of motility are highly downregulated in *Pta* at this same time point compared to growth *in vitro*. Whether these changes truly reflect ecological differences in infection between strains is an interesting question for future studies, but we note that there are reported differences in the ability of *N. benthamiana* to enzymatically process *Psy* and *Pta* flagellin monomers into immunogenic epitopes and mount active immune responses and it may be that *Pta* circumvents immune recognition by downregulating the entire pathway (Naito et al. 2008; Yamamoto et al. 2011; Buscaill et al. 2019). Likewise, these two strains display dissimilar expression patterns with regards to alginate production, as this pathway is upregulated in *Psy* but unchanged to slightly downregulated in *Pta* at the same time point. While alginate production has been proposed to play a role in *P. syringae* tolerance to osmotic and oxidative stress in the apoplast (Chang Woo-Suk et al. 2007; Keith et al. 2003) as well as interfering with plant immune calcium signaling (Aslam et al. 2008; Scrase-Field and Knight 2003), alginate has been observed to make strain-variable contributions to virulence. In *Psy* alginate synthesis gene mutants had decreased apoplastic fitness in bean (Helmann, Deutschbauer, and Lindow 2019). We are not aware of any study directly examining the contributions of alginate to *Pta* virulence.

Taken together, our data paint a picture in which a host plant responds in largely overlapping ways to infection by two independently evolved but closely related compatible pathogens. At least for at 5 hpi and for these two bacterial strains, *N. benthamina* does not appear to discriminate as judged by gene expression outputs, even though infection dynamics and

longer-term symptoms differ between *Pta* and *Psy*. Likewise, even though both pathogens maintain somewhat independent suites of virulence genes, many of these predicted virulence loci are upregulated *in planta*. That host plant gene expression responses largely converge despite underlying differences in virulence factor repertoires likely speaks to both the redundancy of virulence factors as well as the importance of manipulation of system level nodes that pathogens use to overcome plant defense. Ultimately, while there may be many different ways that one can break an egg, eventually the output still converges on an egg getting broken.

## Data Availability

A complete genome assembly for *P. syringae* pv. *tabaci* 11528 genome can be found at Genbank accessions CP042804.1 and CP042805.1. Sequencing reads for Illumina (trimmed) and Nanopore (raw) for this assembly can be found at SRA accessions SRX6691661 and SRX6691662, respectively.

For transcriptome data, raw reads and processed count data can be accessed through GEO (accession GSE201377: For reviewer access, go to https://www.ncbi.nlm.nih.gov/geo/query/acc.cgi?acc=GSE201377 and enter token wjalwaskjrwxxup into the box).

Scripts for recreating figures and analyses can be found on Github at doi.org/10.5281/zenodo.6743815

Supplemental file 1, containing reannotation of type 3 effectors and phytotoxin genes for both strains referenced in this manuscript can be found on FigShare at doi: 10.6084/m9.figshare.20151770.

## Limitations of this Study

We acknowledge that our experimental setup (inoculation of plant leaves by syringe infiltration) differs from the natural routes of infection by both pathogens, which invade through natural openings like the stomata. As such, it is certainly possible that incorporating a more natural route of infection could lead to increased divergence in host responses or in the particular genes that are directly manipulated by pathogen presence. Likewise, natural infection could change the timing of the infection responses to further exacerbate any host expression changes associated with infection after specific time points. We also acknowledge that our comparison group to *in planta* expression data consists of strains under laboratory growth on solid media, and that many housekeeping genes are also differentially upregulated compared to this condition *in planta*. Lastly, we acknowledge the challenge of separating plant transcriptional responses to the pathogen from both wounding responses (given syringe infiltration) as well as circadian ressponses. It is possible that our interpretation results could be affected by this comparison, although we have been careful to limit our interpretations given these limitations throughout the manuscript.

**Acknowledgments**

This material is based upon High Performance Computing (HPC) resources supported by the University of Arizona TRIF, UITS, and Research, Innovation, and Impact (RII) and maintained by the UArizona Research Technologies department. This work was supported in part by the University of Georgia Office of Research as well as the University of Georgia College of Agricultural and Environmental Sciences' Research Office.

## Author Contributions

Conceptualization - DAB, BHK

Methodology - DAB, BHK, AS

Software - MEC

Formal Analysis - MEC

Investigation - DAB, BHK, AS

Resources - DAB, BHK

Data Curation – MEC, DAB

Writing – Original Draft Preparation - MEC, DAB, BHK

Writing – Review & Editing Preparation - MEC, DAB, BHK

Visualization - MEC

Supervision - DAB, BHK

Project Administration - DAB, BHK

Funding Acquisition- BHK

## Materials and Methods

### *Genome Sequencing and Assembly of* Pta

For each genomic DNA extraction used in the assemblies reported here, a sample of this frozen stock was streaked to KB agar plates and single colonies were transferred to 2mL of KB broth and grown overnight at 27$^{o}$C in a shaking incubator at 220rpm after which genomic DNA was isolated. Genomic DNA used for Illumina sequencing was isolated from a 2mL overnight culture via the Promega (Madison, WI) Wizard kit with the manufacturer's protocols. Genomic DNA for Nanopore sequencing was prepared independently using a Circulomics (Baltimore, MD) Nanobind High Molecular Weight DNA extraction kit. RNAse was added as per manufacturer's protocols for all of the genomic isolations where specified.

Genomic DNA was sequenced by SNPsaurus (Eugene, OR) using an Illumina HiSeq 4000 instrument and following their standard workflow for library preparation and read trimming. This workflow uses a Nextera tagmentation kit for library generation, followed by sequencing that generated 150-bp paired-end reads, followed by trimming of adaptors from reads with the computational suite BBDuk (BBMap version 38.41) (9). This workflow generated a total of 2,087,458 trimmed paired reads and 630 Mbp of sequence (~95x coverage). Genomic DNA was also sequenced by the Baltrus lab via an Oxford Nanopore MinION using a R9.4 flowcell, with 1ug of DNA prepared using the LSK-109 kit without shearing or size selecting (other than using the Long Fragment buffer supplied with kit). Reads were called during sequencing using Guppy version 3.2.6 using a MinIT (ont-minit-release 19.10.3) for processing. Nanopore sequencing generated 101,281 reads with an N50 of 6116bp. Sequencing reads for Illumina (trimmed) and Nanopore (raw) can be found at SRA accessions SRX6691661 and SRX6691662, respectively.

Hybrid assembly of all read types was performed using Unicycler version 0.4.8 (Wick et al. 2017). Assembly resulted in a single chromosome: 6,133,558bp and a single 68,162bp plasmid. Both replicons were determined to be circular, and both were rotated per the Unicycler pipeline (8). The genome was annotated using the NCBI PGAP pipeline (Tatusova et al. 2016). Default parameters were used for all software. The assembled chromosome sequence can be found at accession CP042804.1 and the sequence of plasmid pTab1 can be found at CP042805.1.

*Inoculation and sample collection for RNAseq*

Two-week soil germinated *Nicotiana benthamiana* seedlings were transplanted into 4-inch pots with SunGro 3B professional growing mix and fertilized with Peters Professional 20-20-20 water-soluble fertilizer at 1g/L of water. Seedlings we grown in a Conviron Adaptis growth chamber with 12 h light (125 μmol/$m^2$/s) at 26°C and 12 h dark at 23°C for 4 weeks and then transferred to the laboratory plant growth room with 12 h light (35 μmol/$m^2$/s) and ambient room temperature. Plants were 6-13 weeks post-seeding at the time of use.

Samples were collected from two consecutive expanded leaves on each of two plants of the same age, four leaves total. Each of three sample pair sets (T0/T5) were collected as independent experiments on separate days from separate pairs of plants using separately prepared bacterial inoculum. Immediately prior to bacterial inoculation (T0 plant), four 4 mm diameter leaf discs were collected using disposable biopsy punches from each leaf for a total of 16 leaf punches correlating to approximately 2 $cm^2$ leaf tissue and immediately frozen in $LN_2$ until processing.

*Pta* and *Psy* inoculum was prepared directly from fresh KB plate cultures incubated at 28°C (King's B; per 1 L = 20.0 g proteose peptone 3, 0.4 g $MgSO_4 \cdot 7H_2O$, glycerol 10 mL, 2.0 g $K_2HPO_4 \cdot 3H_2O$, 18 g agar), resuspended in 0.25 mM sterile $MgCl_2$ and standardized to $OD_{600}$ 0.5. A 1 mL sample of bacterial inoculum (T0 bacteria) was retained and the bacteria were collected by centrifugation and flash frozen in $LN_2$ until processing. Four leaves (two each on two plants) were fully infiltrated with the cell suspensions using a 1 cc blunt syringe. At 5 hours post-inoculation (T5 plant), a corresponding treatment sample of leaf tissue was collected with biopsy punches as described for T0.

To physically separate the *P. syringae* bacteria from the leaf tissue at 5 hpi (T5 bacteria), we adapted the procedure used by Lovelace et al 2018 for use with *N. benthamiana* leaves. Briefly two *N. benthamian*a leaves each were detached and gently rolled up and inserted into the

barrels of two 20 mL syringes. An RNA stabilizing buffer (De Wit et al. 2012), pH 5.2, was poured into each syringe, which was sealed and vacuum infiltrated at 95 kPa for 2 min, followed by a slow release of the vacuum. Vacuum-infiltration with RNA-stabilizing buffer was conducted twice on inoculated leaves. Excess RNA-stabilizing buffer was decanted and the syringes were placed into 50-ml conical tubes and were centrifuged at 1,000 × *g* for 10 min at 4°C to recover the intercellular wash fluid (O'Leary et al. 2014). The flow-through was concentrated by syringe filtration using a 0.20-µm Micropore Express Plus membrane placed within a removable filtering syringe tip adapter (Millipore, Billerica, MA, U.S.A.). Filters were removed from the adapter and immediately frozen in $LN_2$ until processing.

*RNA Extraction and Sequencing*

Frozen samples were homogenized in 2 mL homogenization tubes with high-density zirconium beads (Glen Mills) using a Geno/Grinder (SPEX SamplePrep) for 1 min at 1,750 Hz with a $LN_2$ chilled sample holder. RNA was extracted using the DirectZol RNA miniprep kit (Zymo Research). RNA samples were DNAse treated with the Turbo DNAse (Thermo-Fisher) followed by cleanup with the Monarch RNA Cleanup Kit (NEB). Reagents were used according to the manufacturer's recommendations.

Plant mRNA sequencing libraries were prepared with the Illumina-compatible KAPA Stranded mRNA-seq Kit (Roche) by the Georgia Genomics and Bioinformatics Core (GGBC). The *Psy* RNA samples were rRNA depleted using the RiboMinus Bacterial kit (Thermo Fisher) and libraries were prepared with the Illumina-compatible KAPA Stranded RNA-seq Kit (Roche) by the GGBC. The *Pta* RNA samples were rRNA depleted using both RiboZero Plant and RiboZero Bacteria (Illumina) in combination and RNA sequencing libraries were prepared in-house using the TruSeq Stranded Total RNA kit (Illumina). Library prep kits were used according to the manufacturer's recommendations.

Indexed libraries were pooled at ratios to target >5 million reads for bacterial RNA samples and 10-20 million reads for plant RNA samples and sequenced at the GGBC. The *Psy* bacterial RNAseq libraries and *Psy*-inoculated Plant mRNAseq samples libraries were pooled and paired-end 75-bp reads were sequenced using the Illumina Nextseq 500 in High-output model. For the pooled *Pta*-inoculated plant RNA samples, paired-end 75-bp reads were sequenced using the Illumina Nextseq 500 in Mid-output model. For the pooled *Pta* bacteria RNA samples, single-end 75-bp reads were sequenced using the Illumina Nextseq 500 in High-output mode.

*RNA-Seq Analysis*

For plant reads, we aligned to the *Nicotiana benthamiana* draft genome sequence v1.0.1 with improved NbD transcriptome (Bombarely et al. 2012; Kourelis et al. 2019) using HISAT2 v2.2.1 and then gene counts were assessed with StringTie v2.2.0 restricting the counts to known transcripts (Pertea et al. 2016). For bacterial reads, bowtie2 v2.4.1 was used for alignment to the *P. syringae* B728a (Genbank: CP000075.1) or *P. amygdali* pv. *tabaci* (Genbank: NZ_CP042804.1 and NZ_CP042805.1) genome and featureCounts from the subread package for gene counts, allowing for overlapping and multimapping partial counts. The sequencing reads from the *in vitro* sample of *Psy* contained too much ribosomal RNA and were not informative

enough for differential expression analysis. Thus, we used previously published (Hockett, Burch, and Lindow 2013) count data from a similar condition (*Psy* grown on KB plates at 20°C) available through the Integrated Microbial Genome website (accessions Gp0060698, Gp0060702, and Gp0060705). We used OMA standalone to determine orthologs between the *Psy* and *Pta* genomes (Altenhoff et al. 2019).

Raw reads and processed count data can be accessed through GEO (accession GSE201377: For reviewer access, go to https://www.ncbi.nlm.nih.gov/geo/query/acc.cgi?acc=GSE201377 and enter token wjalwaskjrwxxup into the box)

We used the R package DESeq2 v1.3.1 (Love, Huber, and Anders 2014) to identify differentially expressed genes based on an adjusted p value of less than 0.01 and an absolute value of $\log_2$ fold change greater than two. As part of the calculation, the threshold on Cook's distance is typically set at 99% quantile of the F(p, m-p) distribution, where p is the number of coefficients being fitted and m is the number of samples according to the DESeq2 manual, but was changed to a 97% quantile for the plant counts to remove additional genes with clear outlier counts among condition replicates. Goseq v3.14 was used for gene ontology enrichment analysis accounting for transcript length bias (Young et al. 2010). Visualization was done with ggplot2 v3.3.5, VennDiagram v1.7.1, viridis v0.6.2, and pheatmap 1.0.12 in R v4.1.2.

## References

Altenhoff, Adrian M., Jeremy Levy, Magdalena Zarowiecki, Bartłomiej Tomiczek, Alex Warwick Vesztrocy, Daniel A. Dalquen, Steven Müller, et al. 2019. "OMA Standalone: Orthology Inference among Public and Custom Genomes and Transcriptomes." *Genome Research* 29 (7): 1152–63.

Aslam, Shazia N., Mari-Anne Newman, Gitte Erbs, Kate L. Morrissey, Delphine Chinchilla, Thomas Boller, Tina Tandrup Jensen, et al. 2008. "Bacterial Polysaccharides Suppress Induced Innate Immunity by Calcium Chelation." *Current Biology: CB* 18 (14): 1078–83.

Baltrus, David A. 2016. "Divorcing Strain Classification from Species Names." *Trends in Microbiology* 24 (6): 431–39.

Baltrus, David A., Honour C. McCann, and David S. Guttman. 2017. "Evolution, Genomics and Epidemiology of Pseudomonas Syringae." *Molecular Plant Pathology* 18 (1): 152–68.

Baltrus, David A., Marc T. Nishimura, Artur Romanchuk, Jeff H. Chang, M. Shahid Mukhtar, Karen Cherkis, Jeff Roach, Sarah R. Grant, Corbin D. Jones, and Jeffery L. Dangl. 2011. "Dynamic Evolution of Pathogenicity Revealed by Sequencing and Comparative Genomics of 19 *Pseudomonas Syringae* Isolates." *PLoS Pathogens* 7 (7): e1002132.

Block, Anna, and James R. Alfano. 2011. "Plant Targets for Pseudomonas Syringae Type III Effectors: Virulence Targets or Guarded Decoys?" *Current Opinion in Microbiology* 14 (1): 39–46.

Bombarely, Aureliano, Hernan G. Rosli, Julia Vrebalov, Peter Moffett, Lukas A. Mueller, and Gregory B. Martin. 2012. "A Draft Genome Sequence of *Nicotiana Benthamiana* to Enhance Molecular Plant-Microbe Biology Research." *Molecular Plant-Microbe Interactions: MPMI* 25 (12): 1523–30.

Buscaill, Pierre, Balakumaran Chandrasekar, Nattapong Sanguankiattichai, Jiorgos Kourelis, Farnusch Kaschani, Emma L. Thomas, Kyoko Morimoto, et al. 2019. "Glycosidase and

Glycan Polymorphism Control Hydrolytic Release of Immunogenic Flagellin Peptides." *Science* 364 (6436). https://doi.org/10.1126/science.aav0748.

Chang Woo-Suk, van de Mortel Martijn, Nielsen Lindsey, Nino de Guzman Gabriela, Li Xiaohong, and Halverson Larry J. 2007. "Alginate Production by Pseudomonas Putida Creates a Hydrated Microenvironment and Contributes to Biofilm Architecture and Stress Tolerance under Water-Limiting Conditions." *Journal of Bacteriology* 189 (22): 8290–99.

Cheung, Alice Y., and Hen-Ming Wu. 2011. "THESEUS 1, FERONIA and Relatives: A Family of Cell Wall-Sensing Receptor Kinases?" *Current Opinion in Plant Biology* 14 (6): 632–41.

Creelman, Robert A., and Rao Mulpuri. 2002. "The Oxylipin Pathway in Arabidopsis." *The Arabidopsis Book / American Society of Plant Biologists* 1 (August): e0012.

Dong, Xiaoyun, Zonglie Hong, Jayanta Chatterjee, Sunghan Kim, and Desh Pal S. Verma. 2008. "Expression of Callose Synthase Genes and Its Connection with Npr1 Signaling Pathway during Pathogen Infection." *Planta* 229 (1): 87–98.

Du, Liqun, Gul S. Ali, Kayla A. Simons, Jingguo Hou, Tianbao Yang, A. S. N. Reddy, and B. W. Poovaiah. 2009. "Ca(2+)/Calmodulin Regulates Salicylic-Acid-Mediated Plant Immunity." *Nature* 457 (7233): 1154–58.

Ellinger, Dorothea, and Christian A. Voigt. 2014. "Callose Biosynthesis in Arabidopsis with a Focus on Pathogen Response: What We Have Learned within the Last Decade." *Annals of Botany* 114 (6): 1349–58.

Fammartino, Alessandro, Francesca Cardinale, Cornelia Göbel, Laurent Mène-Saffrané, Joëlle Fournier, Ivo Feussner, and Marie-Thérèse Esquerré-Tugayé. 2007. "Characterization of a Divinyl Ether Biosynthetic Pathway Specifically Associated with Pathogenesis in Tobacco." *Plant Physiology* 143 (1): 378–88.

Feil, Helene, William S. Feil, Patrick Chain, Frank Larimer, Genevieve DiBartolo, Alex Copeland, Athanasios Lykidis, et al. 2005. "Comparison of the Complete Genome Sequences of Pseudomonas Syringae Pv. Syringae B728a and Pv. Tomato DC3000." *Proceedings of the National Academy of Sciences of the United States of America* 102 (31): 11064–69.

Ferreira, Adriana O., Christopher R. Myers, Jeffrey S. Gordon, Gregory B. Martin, Monica Vencato, Alan Collmer, Misty D. Wehling, et al. 2006. "Whole-Genome Expression Profiling Defines the HrpL Regulon of Pseudomonas Syringae Pv. Tomato DC3000, Allows de Novo Reconstruction of the Hrp Cis Clement, and Identifies Novel Coregulated Genes." *Molecular Plant-Microbe Interactions: MPMI* 19 (11): 1167–79.

Hara, K., M. Yagi, T. Kusano, and H. Sano. 2000. "Rapid Systemic Accumulation of Transcripts Encoding a Tobacco WRKY Transcription Factor upon Wounding." *Molecular & General Genetics: MGG* 263 (1): 30–37.

Heitz, Thierry, Emilie Widemann, Raphaël Lugan, Laurence Miesch, Pascaline Ullmann, Laurent Désaubry, Emilie Holder, et al. 2012. "Cytochromes P450 CYP94C1 and CYP94B3 Catalyze Two Successive Oxidation Steps of Plant Hormone Jasmonoyl-Isoleucine for Catabolic Turnover." *The Journal of Biological Chemistry* 287 (9): 6296–6306.

Helmann, Tyler C., Adam M. Deutschbauer, and Steven E. Lindow. 2019. "Genome-Wide Identification of Pseudomonas Syringae Genes Required for Fitness during Colonization of the Leaf Surface and Apoplast." *Proceedings of the National Academy of Sciences of*

*the United States of America* 116 (38): 18900–910.

Hirano, S. S., A. O. Charkowski, A. Collmer, D. K. Willis, and C. D. Upper. 1999. "Role of the Hrp Type III Protein Secretion System in Growth of Pseudomonas Syringae Pv. Syringae B728a on Host Plants in the Field." *Proceedings of the National Academy of Sciences of the United States of America* 96 (17): 9851–56.

Hirano, Susan S., and Christen D. Upper. 2000. "Bacteria in the Leaf Ecosystem with Emphasis OnPseudomonas Syringae—a Pathogen, Ice Nucleus, and Epiphyte." *Microbiology and Molecular Biology Reviews: MMBR* 64 (3): 624–53.

Hockett, Kevin L., Adrien Y. Burch, and Steven E. Lindow. 2013. "Thermo-Regulation of Genes Mediating Motility and Plant Interactions in Pseudomonas Syringae." *PloS One* 8 (3): e59850.

Hockett, Kevin L., Marc T. Nishimura, Erick Karlsrud, Kevin Dougherty, and David A. Baltrus. 2014. "Pseudomonas Syringae CC1557: A Highly Virulent Strain with an Unusually Small Type III Effector Repertoire That Includes a Novel Effector." *Molecular Plant-Microbe Interactions: MPMI* 27 (9): 923–32.

Keith, Ronald C., Lisa M. W. Keith, Gustavo Hernández-Guzmán, Srinivasa R. Uppalapati, and Carol L. Bender. 2003. "Alginate Gene Expression by Pseudomonas Syringae Pv. Tomato DC3000 in Host and Non-Host Plants." *Microbiology* 149 (Pt 5): 1127–38.

Koo, Abraham J., Caitlin Thireault, Starla Zemelis, Arati N. Poudel, Tong Zhang, Naoki Kitaoka, Federica Brandizzi, Hideyuki Matsuura, and Gregg A. Howe. 2014. "Endoplasmic Reticulum-Associated Inactivation of the Hormone Jasmonoyl-L-Isoleucine by Multiple Members of the Cytochrome P450 94 Family in Arabidopsis." *The Journal of Biological Chemistry* 289 (43): 29728–38.

Kourelis, Jiorgos, Farnusch Kaschani, Friederike M. Grosse-Holz, Felix Homma, Markus Kaiser, and Renier A. L. van der Hoorn. 2019. "A Homology-Guided, Genome-Based Proteome for Improved Proteomics in the Alloploid Nicotiana Benthamiana." *BMC Genomics* 20 (1): 722.

Lam, Hanh N., Suma Chakravarthy, Hai-Lei Wei, Hoangchuong BuiNguyen, Paul V. Stodghill, Alan Collmer, Bryan M. Swingle, and Samuel W. Cartinhour. 2014. "Global Analysis of the HrpL Regulon in the Plant Pathogen Pseudomonas Syringae Pv. Tomato DC3000 Reveals New Regulon Members with Diverse Functions." *PloS One* 9 (8): e106115.

Lee, Hyun Kyung, Seok Keun Cho, Ora Son, Zhengyi Xu, Inhwan Hwang, and Woo Taek Kim. 2009. "Drought Stress-Induced Rma1H1, a RING Membrane-Anchor E3 Ubiquitin Ligase Homolog, Regulates Aquaporin Levels via Ubiquitination in Transgenic Arabidopsis Plants." *The Plant Cell* 21 (2): 622–41.

Lindeberg, Magdalen, Samuel Cartinhour, Christopher R. Myers, Lisa M. Schechter, David J. Schneider, and Alan Collmer. 2006. "Closing the Circle on the Discovery of Genes Encoding Hrp Regulon Members and Type III Secretion System Effectors in the Genomes of Three Model Pseudomonas Syringae Strains." *Molecular Plant-Microbe Interactions: MPMI* 19 (11): 1151–58.

Love, Michael I., Wolfgang Huber, and Simon Anders. 2014. "Moderated Estimation of Fold Change and Dispersion for RNA-Seq Data with DESeq2." *Genome Biology* 15 (12): 550.

Misas-Villamil, Johana C., Izabella Kolodziejek, and Renier A. L. van der Hoorn. 2011. "Pseudomonas Syringae Colonizes Distant Tissues in Nicotiana Benthamiana through Xylem Vessels." *The Plant Journal: For Cell and Molecular Biology* 67 (5): 774–82.

Murtas, Giovanni, Paul H. Reeves, Yong-Fu Fu, Ian Bancroft, Caroline Dean, and George

Coupland. 2003. “A Nuclear Protease Required for Flowering-Time Regulation in Arabidopsis Reduces the Abundance of SMALL UBIQUITIN-RELATED MODIFIER Conjugates.” *The Plant Cell* 15 (10): 2308–19.

Naito, Kana, Fumiko Taguchi, Tomoko Suzuki, Yoshishige Inagaki, Kazuhiro Toyoda, Tomonori Shiraishi, and Yuki Ichinose. 2008. “Amino Acid Sequence of Bacterial Microbe-Associated Molecular Pattern Flg22 Is Required for Virulence.” *Molecular Plant-Microbe Interactions: MPMI* 21 (9): 1165–74.

O’Neill, Erinn M., Tatiana S. Mucyn, Jon B. Patteson, Omri M. Finkel, Eui-Hwan Chung, Joshua A. Baccile, Elisabetta Massolo, Frank C. Schroeder, Jeffery L. Dangl, and Bo Li. 2018. “Phevamine A, a Small Molecule That Suppresses Plant Immune Responses.” *Proceedings of the National Academy of Sciences of the United States of America* 115 (41): E9514–22.

Pertea, Mihaela, Daehwan Kim, Geo M. Pertea, Jeffrey T. Leek, and Steven L. Salzberg. 2016. “Transcript-Level Expression Analysis of RNA-Seq Experiments with HISAT, StringTie and Ballgown.” *Nature Protocols* 11 (9): 1650–67.

Pinot, F., I. Benveniste I, Sala n JP, and F. Durst. 1998. “Methyl Jasmonate Induces Lauric Acid Omega-Hydroxylase Activity and Accumulation of CYP94A1 Transcripts but Does Not Affect Epoxide Hydrolase Activities in Vicia Sativa Seedlings.” *Plant Physiology* 118 (4): 1481–86.

Prost, Isabelle, Sandrine Dhondt, Grit Rothe, Jorge Vicente, Maria José Rodriguez, Neil Kift, Francis Carbonne, et al. 2005. “Evaluation of the Antimicrobial Activities of Plant Oxylipins Supports Their Involvement in Defense against Pathogens.” *Plant Physiology* 139 (4): 1902–13.

Sanadhya, Payal, Anil Kumar, Patricia Bucki, Nathalia Fitoussi, Mira Carmeli-Weissberg, Menachem Borenstein, and Sigal Brown-Miyara. 2021. “Tomato Divinyl Ether-Biosynthesis Pathway Is Implicated in Modulating of Root-Knot Nematode Meloidogyne Javanica’s Parasitic Ability.” *Frontiers in Plant Science* 12 (August): 670772.

Schellenberg, Barbara, Christina Ramel, and Robert Dudler. 2010. “Pseudomonas Syringae Virulence Factor Syringolin A Counteracts Stomatal Immunity by Proteasome Inhibition.” *Molecular Plant-Microbe Interactions: MPMI* 23 (10): 1287–93.

Scrase-Field, Sarah A. M. G., and Marc R. Knight. 2003. “Calcium: Just a Chemical Switch?” *Current Opinion in Plant Biology* 6 (5): 500–506.

Seo, Pil Joon, Jungmin Park, Mi-Jeong Park, Youn-Sung Kim, Sang-Gyu Kim, Jae-Hoon Jung, and Chung-Mo Park. 2012. “A Golgi-Localized MATE Transporter Mediates Iron Homoeostasis under Osmotic Stress in Arabidopsis.” *Biochemical Journal* 442 (3): 551–61.

Studholme, David J., Selena Gimenez Ibanez, Daniel MacLean, Jeffery L. Dangl, Jeff H. Chang, and John P. Rathjen. 2009. “A Draft Genome Sequence and Functional Screen Reveals the Repertoire of Type III Secreted Proteins of Pseudomonas Syringae Pathovar Tabaci 11528.” *BMC Genomics* 10 (August): 395.

Sun, Suli, Changyou Liu, Canxing Duan, and Zhendong Zhu. 2021. “Wildfire, a New Bacterial Disease of Mung Bean, Caused by Pseudomonas Syringae Pv. Tabaci.” *Journal of Plant Pathology: An International Journal of the Italian Phytopathological Society* 103 (2): 649–53.

Tatusova, Tatiana, Michael DiCuccio, Azat Badretdin, Vyacheslav Chetvernin, Eric P. Nawrocki, Leonid Zaslavsky, Alexandre Lomsadze, Kim D. Pruitt, Mark Borodovsky,

and James Ostell. 2016. “NCBI Prokaryotic Genome Annotation Pipeline.” *Nucleic Acids Research* 44 (14): 6614–24.

Vinatzer, Boris A., Gail M. Teitzel, Min-Woo Lee, Joanna Jelenska, Sara Hotton, Keke Fairfax, Jenny Jenrette, and Jean T. Greenberg. 2006. “The Type III Effector Repertoire of Pseudomonas Syringae Pv. Syringae B728a and Its Role in Survival and Disease on Host and Non-Host Plants.” *Molecular Microbiology* 62 (1): 26–44.

Wang, Qing, Yali Sun, Fang Wang, Pei-Cheng Huang, Yinying Wang, Xinsen Ruan, Liang Ma, Xin Li, Michael V. Kolomiets, and Xiquan Gao. 2021. “Transcriptome and Oxylipin Profiling Joint Analysis Reveals Opposite Roles of 9-Oxylipins and Jasmonic Acid in Maize Resistance to Gibberella Stalk Rot.” *Frontiers in Plant Science* 12 (September): 699146.

Wick, Ryan R., Louise M. Judd, Claire L. Gorrie, and Kathryn E. Holt. 2017. “Unicycler: Resolving Bacterial Genome Assemblies from Short and Long Sequencing Reads.” *PLoS Computational Biology* 13 (6): e1005595.

Wu, Shu-Wei, Ritesh Kumar, Arya Bagus Boedi Iswanto, and Jae-Yean Kim. 2018. “Callose Balancing at Plasmodesmata.” *Journal of Experimental Botany* 69 (22): 5325–39.

Xiao, Y., and S. W. Hutcheson. 1994. “A Single Promoter Sequence Recognized by a Newly Identified Alternate Sigma Factor Directs Expression of Pathogenicity and Host Range Determinants in Pseudomonas Syringae.” *Journal of Bacteriology* 176 (10): 3089–91.

Xin, Xiu-Fang, Brian Kvitko, and Sheng Yang He. 2018. “Pseudomonas Syringae: What It Takes to Be a Pathogen.” *Nature Reviews. Microbiology* 16 (5): 316–28.

Yamamoto, Masanobu, Mayumi Ohnishi-Kameyama, Chi L. Nguyen, Fumiko Taguchi, Kazuhiro Chiku, Tadashi Ishii, Hiroshi Ono, Mitsuru Yoshida, and Yuki Ichinose. 2011. “Identification of Genes Involved in the Glycosylation of Modified Viosamine of Flagellins in Pseudomonas Syringae by Mass Spectrometry.” *Genes* 2 (4): 788–803.

Young, Matthew D., Matthew J. Wakefield, Gordon K. Smyth, and Alicia Oshlack. 2010. “Gene Ontology Analysis for RNA-Seq: Accounting for Selection Bias.” *Genome Biology* 11 (2): R14.

Yuan, Peiguo, Kiwamu Tanaka, and B. W. Poovaiah. 2021. “Calmodulin-Binding Transcription Activator AtSR1/CAMTA3 Fine-Tunes Plant Immune Response by Transcriptional Regulation of the Salicylate Receptor NPR1.” *Plant, Cell & Environment* 44 (9): 3140–54.

Zhang, Lei, Liqun Du, and B. W. Poovaiah. 2014. “Calcium Signaling and Biotic Defense Responses in Plants.” *Plant Signaling & Behavior* 9 (11): e973818.

Zheng, Zuyu, Synan Abu Qamar, Zhixiang Chen, and Tesfaye Mengiste. 2006. “Arabidopsis WRKY33 Transcription Factor Is Required for Resistance to Necrotrophic Fungal Pathogens.” *The Plant Journal: For Cell and Molecular Biology* 48 (4): 592–605.

**Supplemental**

**Supplemental Table 1** (excel file). Output from differential expression analysis for DESeq2 for *Nicotiana benthamiana* genes in response to inoculation with *Psy* or *Pta*.

**Supplemental Table 2** (excel file). Output from differential expression analysis for DESeq2 for *Psy* contrasting *in vitro* and *in planta* conditions.

**Supplemental Table 3** (excel file). Output from differential expression analysis for DESeq2 for *Pta* contrasting *in vitro* and *in planta* conditions.

**Supplemental Table 4** (excel file). Output from OMA indicating orthologs between *Psy* and *Pta* genomes.

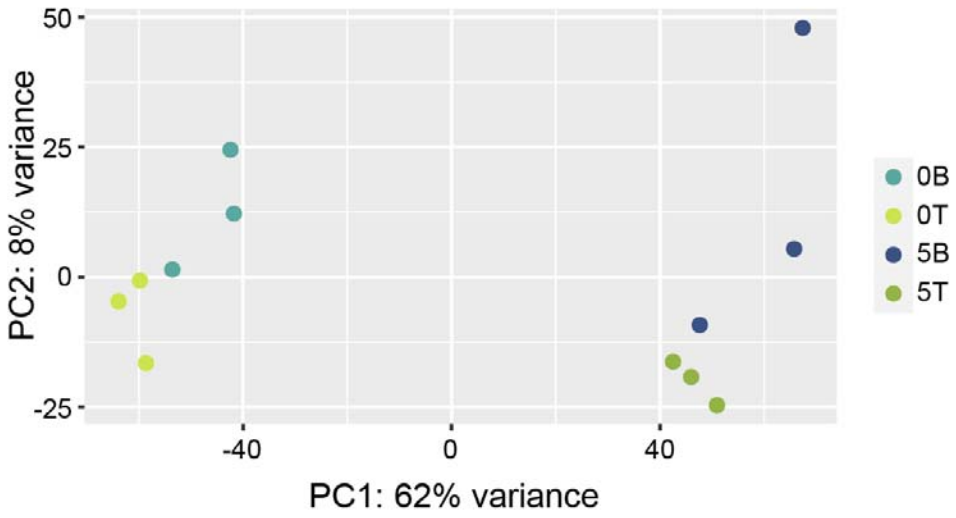


**Supplemental Figure 1**. A principal component analysis plot depicting the three biological replicates for each of the four conditions sampled from *Nicotiana benthamiana* in the RNA-seq analysis. 0B, uninoculated; 0T, uninoculated; 5B, 0B plants 5 hpi with *Psy*, 5T, 0T plants 5 hpi with *Pta*.

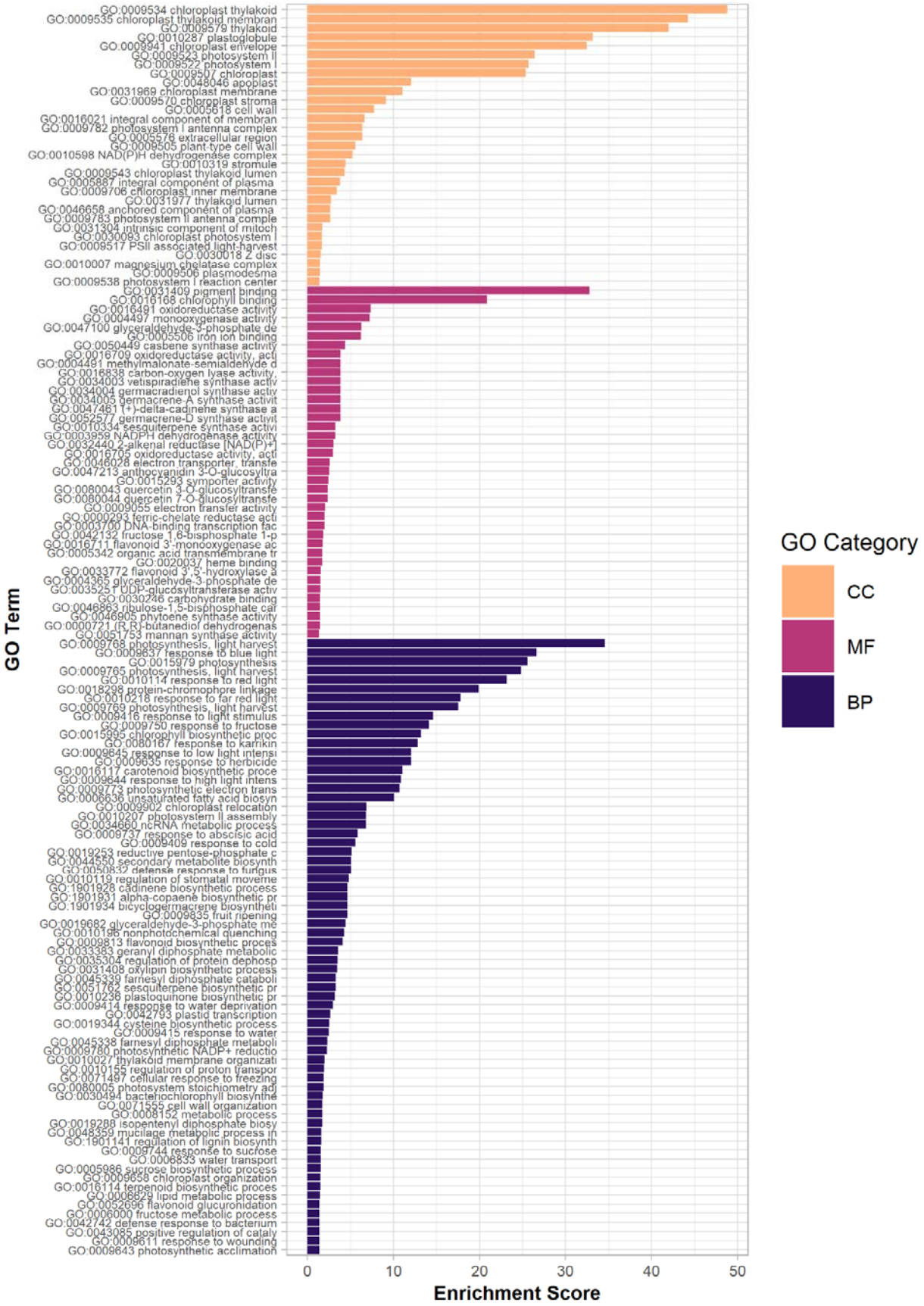

**Supplemental Figure 2**. All enriched gene ontology terms for the differentially expressed genes shared in the responses to inoculation with *Psy* or *Pta* at 5 hpi. GO terms were considered enriched for an adjusted *p* value<0.05. CC, cellular component; MF, molecular function; BP, biological processes.

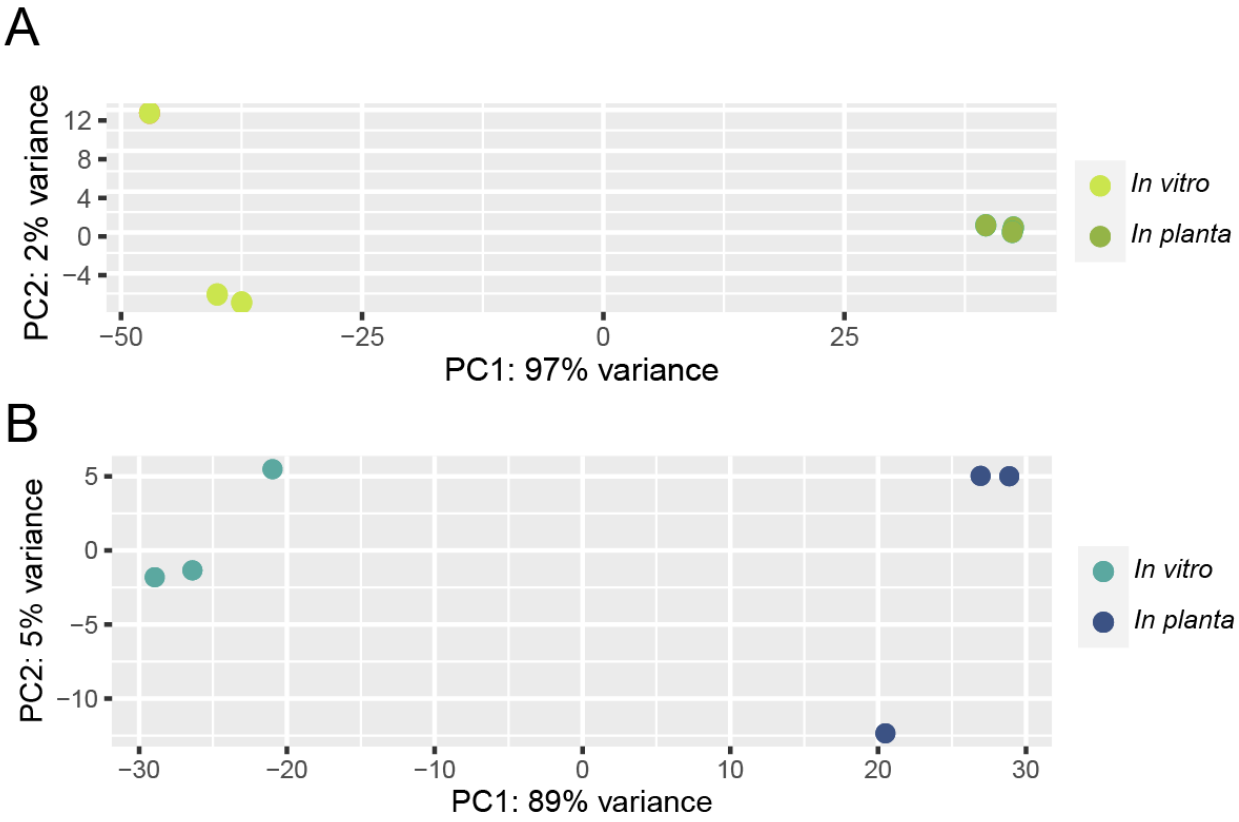


**Supplemental Figure 3.** A principal component analysis plot depicting the three biological replicates for each of the four conditions sampled in the RNA-seq analysis of A) *Pta* and B) *Psy*.

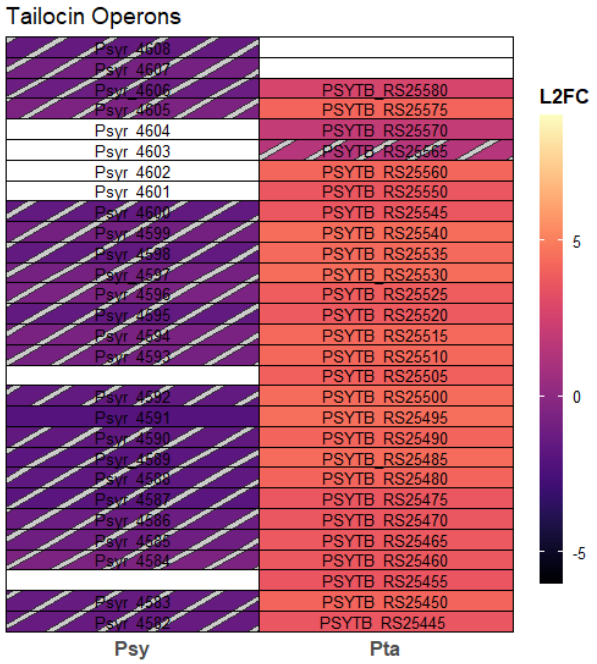


**Supplemental Figure 4.** Differential expression of tailocin operons in *Psy* and *Pta in planta*. Striped boxes indicate genes that are significant for different thresholds: adjusted p value<0.05 and no minimum $\log_2$ fold change (L2FC). White boxes indicate no ortholog present or, when labeled with a locus ID, orthologs that are not differentially expressed.